Original Article | *Peer Reviewed* | Open Access

Combinatorial impact of Chelerythrine and DADS in the restoration of liver physiology during carcinogenic exposure in mice (*Mus musculus*)

Soumosish Paul[1*] and Gobinda Chandra Sadhukhan[2]

Check for updates

[1]Department of Zoology, Acharya Prafulla Chandra College, New Barrackpore, Kolkata-700131, West Bengal, India; [2]Rtd. Director, UGC-HRDC at Jadavpur University, Kolkata – 700032, India

E-mail/Orcid Id:

SP, ✉ soumosish@apccollege.ac.in, ⓘ https://orcid.org/0000-0002-7239-0971; *GCS,* ✉ gobindasadhukhan@gmail.com

Abstract: Investigation of the efficacy of the combined drugs chelerythrine and DADS in restoring chemically induced hepatocellular carcinoma in Swiss albino mice. 4-6 week-old mice were considered for experimentation. The genotoxic carcinogen para-induced liver cancer--dimethyl-amino azobenzene along with nongenotoxic promoter carcinogen phenobarbital exposure. During the study, animals were co-treated with 100mg/kg body weight DADS and 5mg/kg body weight chelerythrine individually or in combination for 120 days. Bioparametric enzymatic assays of ALT, AST, ALKP, and GGT were performed. The estimation of TBARS, analysis of bone marrow chromosomal abnormalities, sperm head anomalies, and histopathological tissue structure in the co-treated group followed studies. An increase in enzymatic activities of plasma ALT, AST, ALKP, and GGT was observed after carcinogen exposure. Individual treatment of chelerythrine and DADS restored the activities mentioned above to some extent, although combined drugs successfully maintained the enzymatic activities in plasma. Changes in bone marrow chromosomal morphology and sperm head anomalies after carcinogen exposure were prevented in the individual and, most significantly, after combined drug therapy. Histopathological analysis of liver tissue of both male and female mice also demonstrated the preservation of tissue structures in the treated group, most significantly in the combined treatment, even after PB+P-DAB exposure. Chelerythrine and DADS individually protected liver tissue to a certain extent from the tumorigenic toxic effect of PB+P-DAB exposure. The combination of DADS and chelerythrine successfully guarded the tissue from any corrosive, carcinogenic impact and thus instigated further consideration as an effective alternative therapy against chemically induced hepatocarcinoma.

Introduction

Hepatocellular carcinoma (HCC) is a cancer that arises from the liver. It is known as primary liver carcinoma. The liver comprises different cell types, such as hepatocytes, epithelial cells, bile ducts, endothelial cells in blood vessels, and fat-storing cells. Among them, liver hepatocytes alone make up 80% of liver tissue (Kmieć, 2001). Thus, the majority of primary hepatocellular carcinoma arises from hepatocytes (Feliberti and Wagman, 2006; Fielding, 2006). Liver cancer often refers to cancer that has spread to the liver, originating from other organs as metastatic liver cancer or hepatocellular carcinoma. This is one of the fifth most common cancers worldwide (Andrade et al., 2009; Madhu et al., 2022; Saha et al., 2023). The geographic areas at higher risk are located in China and eastern Asia, middle Africa, and some countries of western Africa. Lower incidences are encountered in Japan, Europe, and America, but this incidence is still rising in part mostly because of the high level of hepatitis C virus infection (El-Serag, 2012; Chatterjee et al., 2021). HCC is an

epithelial tumor that generally develops in the setting of chronic hepatitis or cirrhosis (Gomes et al., 2013; Wangensteen et al., 2018), where there is continuous inflammation and regeneration of hepatocytes. Mechanisms of hepatocarcinogenesis are not completely understood, but like most solid tumors, the development and progression of HCC are believed to be caused by the accumulation of genetic changes resulting in altered expression of cancer-related genes, such as oncogenes or tumor suppressor genes, as well as genes involved in different regulatory pathways (Thorgeirsson and Grisham, 2002; Petruczynik et al., 2019; Mehta et al., 2023; Kulkarni et al., 2023). To understand the mechanism of liver cancer development, several models have been designed using carcinogenic chemicals, hormones, and viruses (Marszałek, 2000; Moon et al., 2022). This process is almost always multistep. During the long period of cancer development, discrete cells or cell populations acquire various properties that make-up cancer (Marszałek, 2000; Rami et al., 2023). The hepatocarcinogenic models are useful in identifying and analysing the preneoplastic and neoplastic alterations during HCC (Marszałek, 2000). The remarkable similarities between many models with different carcinogens in animals and humans suggest the importance of such studies in understanding the molecular basis of liver cancer development.

Based on this theoretical foundation, we treated Swiss albino mice (*Mus musculus)* with phenobarbital and para-dimethyl-aminoazobenzene to study the hepatocarcinogenesis mechanisms. Phenobarbital (PB) is a mitogenic non-genotoxic carcinogen, while para-dimethylaminoazobenzene (P-DAB) is a genotoxic carcinogen (Bhattacharya and Khuda-Bukhsh, 2004). We found that PB, in combination with P-DAB induces hepatotoxicity and tumor generation in mice. Using this PB+P-DAB treated group. Our objective was to identify novel chemopreventive agents and their combined treatment procedures with traditional medicine for successful ameliorative means during HCC development.

Materials and Methods
Animals

A group of 100 healthy Swiss Albino mice (50 males and 50 females), with weights of 20-25g, were selected as models for the *in-vivo* studies of the experimental work. The experiment was performed separately for female and male animals to study the impact associated with sex bias, if any. A group of 10 animals was considered as a control separately for the

female as well as male experimental set. An alternative group of 10 animals was set to observe the extent of damage for either sex at the morphological, physiological, histological, biochemical, cytogenetic, and molecular levels after carcinogenic exposure. To determine the efficacy of the treatment, a set of groups was co-treated with 50,100,150 mg/kg body weight DADS, an active organosulphur component of garlic and another set of groups was co-treated with 2.5, 5, 7.5 mg/kg body weight chelerythrine, an active component of *Chelidonium majus*. After optimization of the dose, further experiments were processed with 100mg/kg body weight DADS and 5mg/kg body weight chelerythrine to determine the effect of combination treatment. The experiment was conducted for 120 days.

Experimental animals were bred in-house and maintained at 27 ± 2^0C, 44–56% relative humidity, and a 12 h light/darkness cycle with free access to food and water in a cross-ventilated room. Experiments were designed following the ethical guidelines of the animal ethics committee of Vidyasagar College, University of Calcutta, to minimize animal suffering and to use the minimum number required for statistical validity.

Different sets of mice were used for the experimental analysis

1. Control,
2. PB+P-DAB,
3. PB+P-DAB+CHEL,
4. PB+P-DAB+DADS,
5. PB+P-DAB+CHEL+DADS

[PB=Phenobarbital, P-DAB= Paradi-methyl-aminoazobenzene. CHEL= Chelerythrine, DADS= Diallyl disulfide]

Instruments and Reagents

ALT, AST, ALKP, and GGT measurement kits were obtained from TECO Diagnostics, CA, USA. Phenobarbital and paradigm ethyal-aminoazobenzene, eosin, hematoxylin, and all other fine chemicals were purchased from Sigma-Aldrich Corporation, St. Louis, MO, USA. Several apparatus were used to perform experimental work, such as a cooling centrifuge (Remi C24BL, Remi, Goregaon (East), Mumbai, India); UV-VIS Spectrophotometer (UV mini1240, Shimadzu Corp. Kyoto Japan); Spinwin (Tarsons Pvt. Ltd. New Delhi India); Microscope (Olympus, Tokyo, Japan)

Analysis of biochemical indices

After a stipulated period of experimental schedule, enzymatic activities of ALT, AST, ALKP, and GGT were analyzed as biomarkers for tissue biochemistry. ALT, AST, ALKP and GGT activities were performed

following the kit protocol (TECO Diagnostics, CA, USA). For ALT and AST, the absorbance was measured at 320nm for 30-second intervals up to 2 min. In ALKP analysis, absorbance was determined at 405nm for 30-sec intervals. The value was calculated after determining the mean absorbance change per minute. The GGT assay measured absorbance at 405nm for 60-second intervals.

Quantification of TBA reactive substances

Determination of TBARS content was initiated by the addition of 1ml of 10mM Tris–HCl buffer (pH 7.4) to 0.4mg of membrane protein (in 0.9% saline, pH 7.4). Then 2ml TBA–TCA reagent (15% TCA and 0.4% TBA) was added to it, and the reaction mixture was boiled for 15min. After centrifugation, the absorbance of clear aqueous supernatant was measured at 532nm. Values were quantified considering the molar extinction coefficient as 1.56×10^5 $M^{-1}cm^{-1}$ and were expressed in moles/mg protein.

Determination of cytogenetic parametric

In bone marrow chromosomal analysis, 0.04% colchicine solution (1ml/100 gm. body weight) was administered intraperitoneally to the mice, and the animals were sacrificed within 45-60 minutes of injection. Then, the femur was dissected, the marrow was flushed with prewarmed 0.9% KCl solution, and the mixture was incubated in a water bath at 37^0C for 10 minutes. Next, the femur was centrifuged for 10 minutes at 1000 rpm. The supernatant was discarded, and the pellet was mixed with an aceto-alcohol (1:3) solution. Finally, slides were prepared by conventional flame dye technique, and Giemsa stained chromosomes the next day.

The analysis of sperm head anomalies (SHA) was initiated by dissecting the epididymis from each side of the respective groups of mice, and its inner content was squeezed out into 0.87% physiological saline. The content was thoroughly cleared from vas deferens, tissue remnants, and lipid droplets, filtered through a silken cloth, and dropped on grease-free clean slides. Later, slides were allowed to air dry and then stained by dilute Giemsa for microscopic observation.

The study of histological structure

The liver was dissected from the respective group of mice, and the paraffin block was prepared following the standard procedure. The tissue was sectioned and stretched on the Mayers albumin-coated slide. Finally, sections were stained following the double staining procedure and were observed under amicroscope.

Flow Chart of experimental pathways

Morphometric analysis for dose selection of the said drugs →Study of different biochemical indices like ALT→AST→ALKP → GGT→ TBARS analysis for toxicity test of the said drugs → performed cytogenetic parameters like bone marrow analysis and Sperm head abnormality test → Histological analysis to establish the correlation with morphometric study.

Statistical analysis

The sample mean and SEM were calculated using the standard method. The Student's t-test determined differences among treatment groups with the carcinogen-exposed group. Correlational, parametric, and other statistical analyses were performed in Microsoft Excel. The significance of the studies was determined using GraphPad Instat software (Graph Pad, La Jolla, CA, USA). Variations were considered statistically significant when $p < 0.05$.

Results

Tumour regression occurred after DADS and chelerythrine treatment in PB+P-DAB exposed mice

Swiss albino mice were exposed to PB and p-DAB to induce hepatocarcinoma. Liver morphology demonstrated the development of liver tumors (Figure 1E and F; marked by white arrows) in male and female mice. Our data suggested a significant enhancement in tumor number/4x4mm² tissue surface area and a corresponding increase in the size of liver tissue as reflected by the liver weight/ body weight ratio in males (Figure 1E and F) and females (Figure 1B and D) mice after 120 days of PB+p-DAB exposure. To analyze the efficacy of the tissue-protective drug, carcinogen-exposed male and female mice were co-treated with 50,100, or 150 mg/kg body weight of DADS (Figure 1C and D) as well as 2.5,5, or 7.5 mg/kg body weight of chelerythrine (Figure 1A and B). Data suggested effective protection from tumor generation and maintenance of liver weight/ body weight ratio significantly in the 100mg/kg body DADS (Figure 1C and D) and 5mg/kg body weight chelerythrine (Figure 1A and B) co-treated group in both male and female mice. Further, an increase in dose to 150 mg/kg body weight DADS and 7.5 mg/kg body weight of chelerythrine did not show any significant change in the continuation of the treatment. Experimental analysis was extended with the combination of selected doses of DADS and chelerythrine to explore the effects of combination treatment. The average length of tumor nodules in mm displayed a reduction of tumorigenic effect after single and most significantly in the combined drug-treated group (Figures G and H). Results revealed that males are much more affected than female mice in carcinogenic exposure, as it was portrayed by a distinct
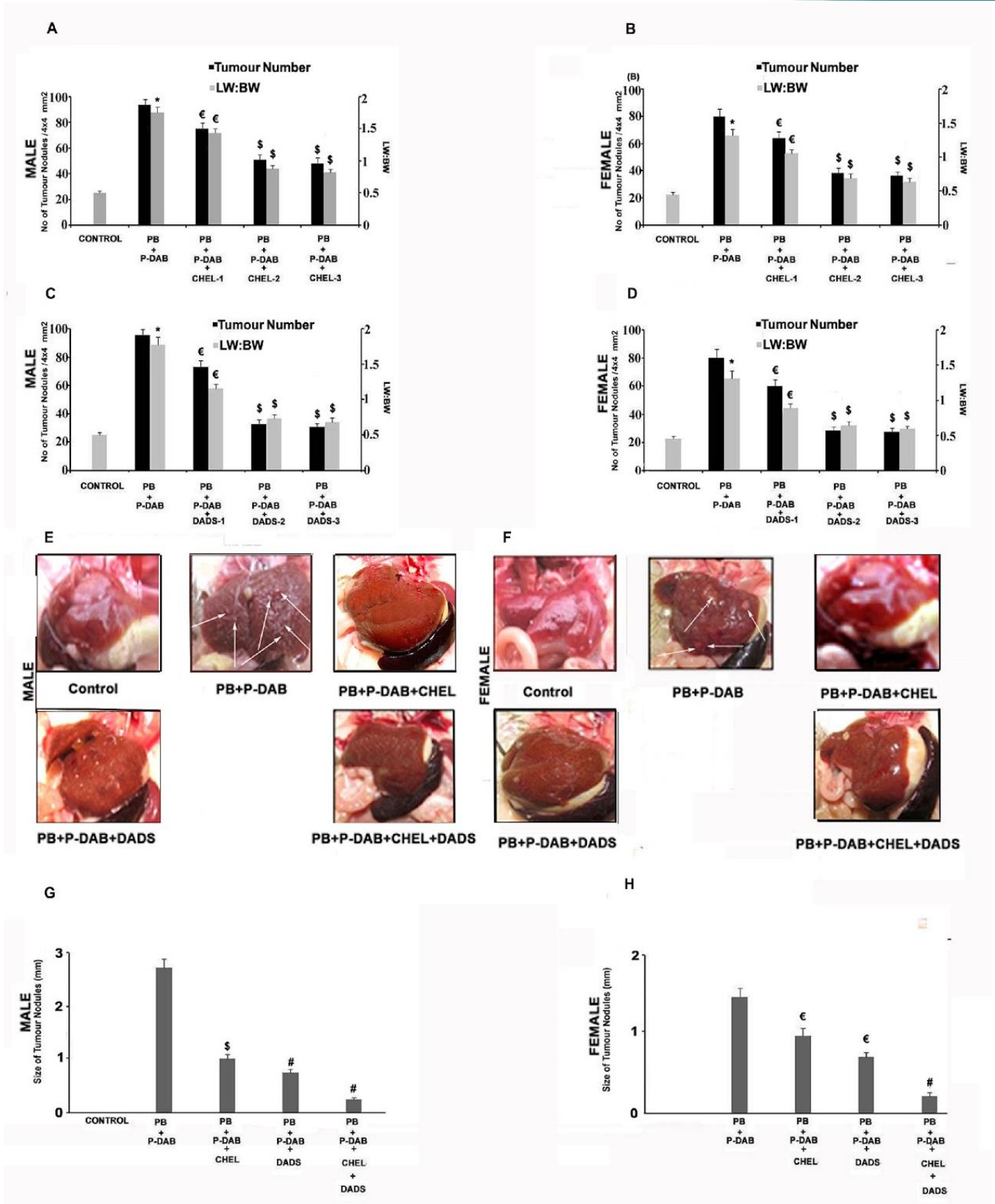
Figure 1. Tumor regression occurred after DADS and chelerythrine treatment in PB+P-DAB exposed mice. PB+P-DAB exposed male (A) and female (B) mice were co-treated with 5mg/kg body weight chelerythrine and 100mg/kg body weight DADS were co-administered to PB+P-DAB exposed male (C) and female (D) mice. The status of liver cancer was represented by the number of tumor nodules/4x4 mm2 and liver weight: body weight ratio. Liver morphology was estimated in male (E) and female (F) mice. Tumors were marked by white arrows in both male (C) and female (D) mice.

increase in tumor size and number in male mice (Figure G) concerning their corresponding female group (Figure H). The study pointed out effective protection to a similar level both in male and female carcinogen-exposed mice after DADS and chelerythrine therapy (Figures G and H).

The effects of the optimized dose of 100mg/kg body weight DADS and 5mg/kg body weight chelerythrine as well as in combination, were estimated in male (E) and female (F) mice. The direct impact upon tumorigenic properties was estimated by determining the size of tumor nodules (mm) in individual 100mg/kg body weight DADS, 5mg/kg body weight chelerythrine, and combined drug co-treatment of PB+P-DAB exposed male (G) and female (H) group of mice. *p<0.01 vs control, €p<0.05, #p<0.02, $p<0.01 vs PB+P-DAB exposed group.

Status of enzymatic biomarkers of hepatocellular carcinoma after DADS and chelerythrine co-treatment in PB+P-DAB exposed mice

Alkaline phosphatase is a hydrolase enzyme that dephosphorylates biomolecules such as nucleotides, proteins, and alkaloids (AL-Auqbi et al., 2012). It is a very useful prognostic serum biomarker with wide applications for predicting hepatocellular carcinoma (Xu et al., 2014). Results indicated enhanced ALKP activity in male mice (Figure 2A) and female mice (Figure 2C) after PB+P-DAB introduction. Individual co-treatment with 100mg/kg body weight DADS and 5mg/kg body weight chelerythrine inhibited ALKP activation to such an extent even after PB+P-DAB exposure both in male (Figure 2A) and female (Figure 2C) mice. The combination of chelerythrine and DADS effectively maintained the enzymatic activity towards the control level in females (Figure 2C) and specifically in male mice, as depicted by Figure 2A. The correlation between tumor size(mm) and ALKP activities of carcinogen-exposed and drug-treated groups was represented in Figure 2B (male mice) and Figure 2D (female mice). Data suggested a notable correlation between ALKP activity and the tumor size (mm) in the respective group of male (Figure 2B: $R^2=0.779$) and female (Figure 2D: $R^2=0.5348$) mice.

Gamma-glutamyl transferase (GGT), the cell surface enzyme involved in cellular glutathione homeostasis, is often significantly increased in liver tumors. Its role in tumor progression, invasion, and drug resistance has been repeatedly suggested. Analysis demonstrated a significant increase in GGT activity in females (Figure 2G) and most effectively, in male mice (Figure 2E) after carcinogen exposure. 5mg/kg body weight chelerythrine and 100mg/kg body weight DADS individually prevented enzyme activity of GGT to some extent concerning only the PB+P-DAB exposed group of males (Figure 2E).

and female (Figure 2G) mice. The combination of the drugs maintained GGT activity nearly about the control level evenly in either set of mice (Figure 2E and G). The correlation between tumor size (mm) and GGT activities of carcinogen-exposed and drug-treated groups was represented in Figure 2F for male mice and Figure 2H for female mice. Data suggested an effective correlation between GGT activity and tumor size (mm) in the presence or absence of chelerythrine and DADS co-treatment in the PB+P-DAB exposed group significantly in the male mice (Figure 2F: $R^2=0.8968$). The result also demonstrated a distinct correlation in a female mouse (Figure 2H: $R^2=0.6158$) between the size of the developed tumor (mm) and GGT activity.

In ALKP analysis, a working reagent was prepared according to the kit protocol. Then, 20µl of serum was taken from each sample and mixed with the working reagent. The reaction mixture was incubated for 30 sec, and absorbance was measured at 405nm for 30 sec intervals. Values were represented in U/L. The size of the tumor nodules (mm) and ALKP activity of PB+P-DAB exposed, individual as well, and combined drug co-treated groups were demonstrated for male (A) and female (C) mice. Correlation between ALKP activity and the size of the tumor (mm) of respective groups was also exhibited both for male (B) and female (D) animals. Following the GGT protocol, 100µl of the serum sample was added to the prepared working reagent during the kit assay. Next, the mixture was incubated for 60 sec, and absorbance was measured at 405nm. Values were represented in U/L. The size of the tumor nodules (mm) and ALKP activity of PB+P-DAB exposed, individual as well, and combined drug co-treated groups were demonstrated for male (E) and female (G) mice. Correlation between GGT activity and the size of the tumor (mm) of respective groups was also exhibited both for male (F) and female (H) animals. The shaded area represented the control value of the experiment. *p<0.01 vs. control, @p<0.05, #p<0.02, $p<0.01 vs. PB+P-DAB exposed group.

Analysis of ALT and AST activities in hepatocellular carcinoma after DADS and chelerythrine treatment in PB+P-DAB exposed mice

Tumor generation damages the liver function and leads to the release of alanine transaminase (ALT). This transamination regulatory enzyme catalyzes the transfer of an amino group from L-alanine to α-ketoglutarate and aspartate transaminase (AST). This amino-
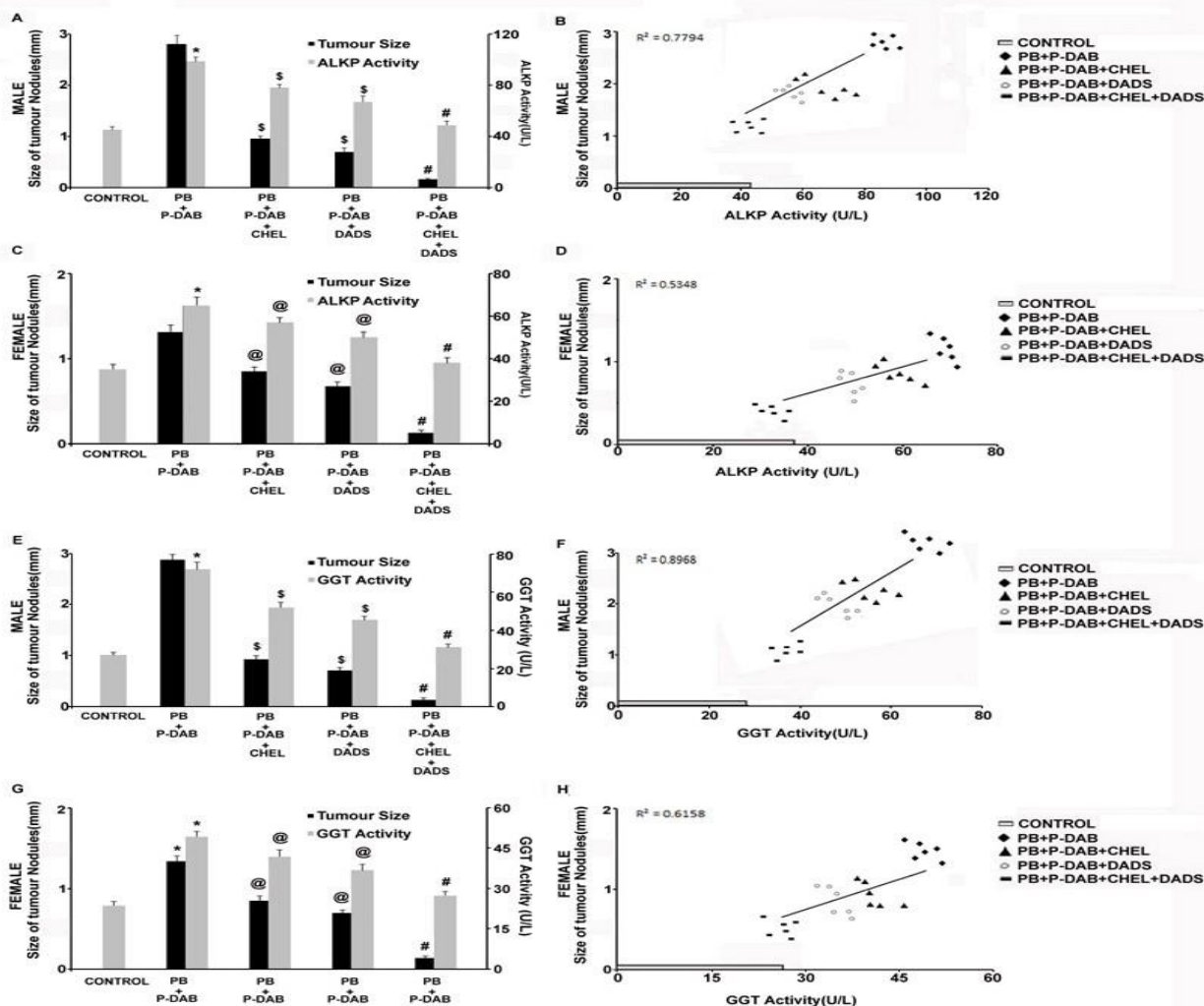
Figure 2. Status of cellular biochemical parameters after DADS and chelerythrine co-treatment. Enzymatic biomarkers like ALKP (A, B, C, D) and GGT (E, F, G, H) activities were analyzed as an indicator of the preservation of liver physiology in DADS and chelerythrine co-treatment of PB+P-DAB exposed mice.

transferase catalyzes the inter-conversion of aspartate and α-ketoglutarate to oxaloacetate and glutamate in the biological system (Singh et al., 2011). An increase in ALT and AST activities in plasma indicates liver dysfunction (Hyder et al., 2013).

The data showed enhanced ALT and AST activities in female (Figure 3C and G) and male (Figure 3A and E) mice after PB+P-DAB exposure. Compared to the carcinogen-exposed group, co-treatment with DADS and chelerythrine individually maintained these enzymatic activities to a certain level. The combination of DADS and chelerythrine effectively reduced the activities of such enzymes towards the basal level concerning control mice (Figure 3A, 3C, 3E, and 3G). Correlation analysis suggested a direct impact of tumor development on liver physiology, as depicted by the increased plasma ALT (Figure 3B: $R^2=0.8665$ in male and Figure 3D: $R^2=0.5661$ in female mice) and AST (Figure 3F: $R^2=0.91$ in male mice and Figure 3H;

$R^2=0.83$ in female mice) activities. A close correlation of tumor number with plasma AST and ALT activities is more significant in male mice (Figure 3B and F) than in the corresponding female group

(Figure 3D and H) after carcinogen exposure, confirming the susceptibility of male mice to chemically induced hepatocarcinoma. Reduction in enzymatic activities concomitant with the protection from tumor development after DADS and chelerythrine co-treatment, individually and specifically in combination, further demonstrated the efficacy of drug treatment against carcinogenic exposure (Figure 3A, 3B and 3E, 3F).

Analysis of ALT and AST activities in hepatocellular carcinoma after DADS and chelerythrine treatment in PB+P-DAB exposed mice

Tumor generation damages the liver function and leads to the release of alanine transaminase (ALT). This transamination regulatory enzyme catalyzes the transfer of an amino group from L-alanine to α- ketoglutarate
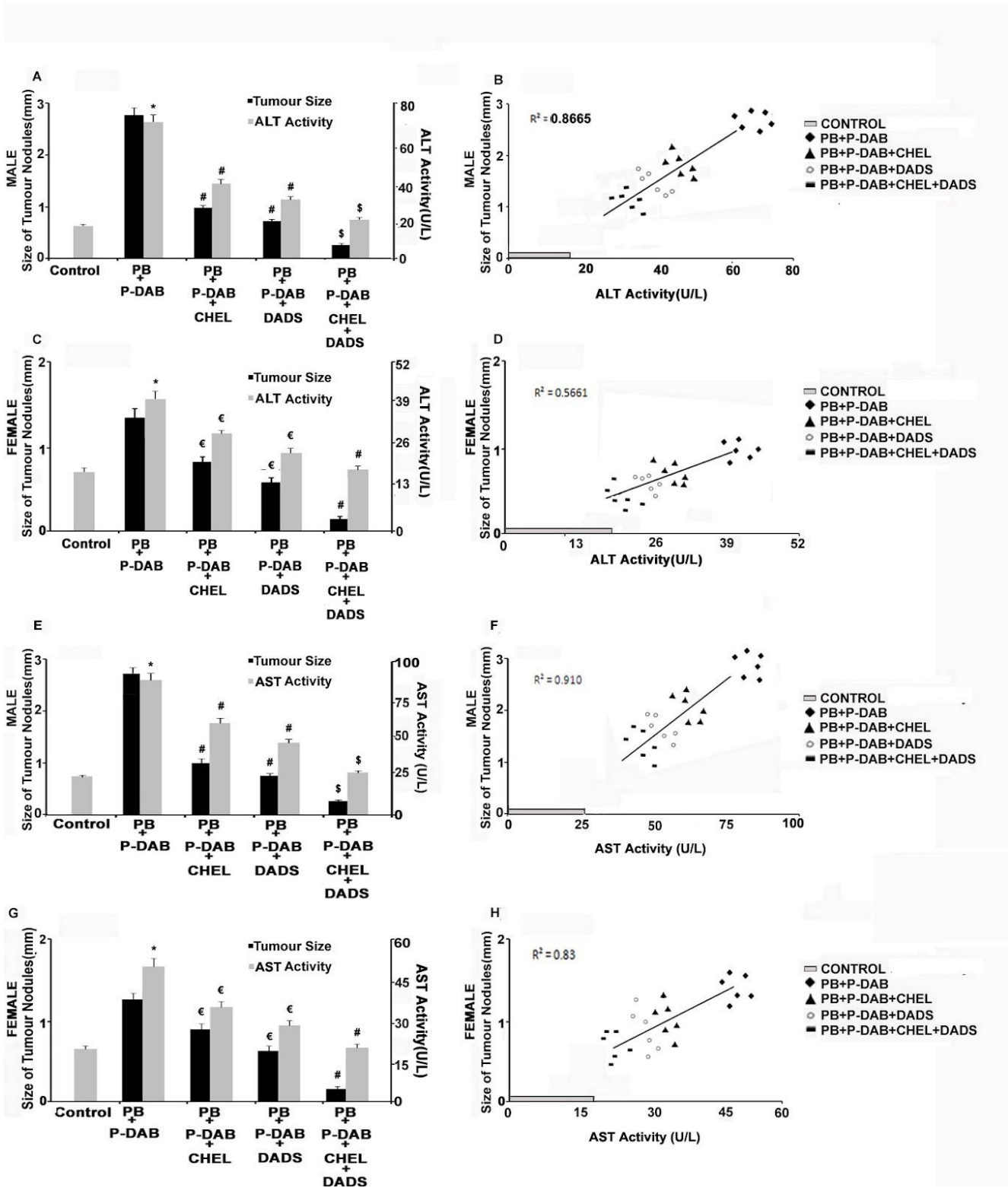
Figure 3. ALT (A, B, C, D) and AST (E, F, G, H) activities were analyzed as a biomarker of hepatocellular biochemistry in DADS and chelerythrine co-treated groups with respective untreated PB+P-DAB exposed mice. In the experimental procedure during the ALT assay reagent 2 and reagent 1 were mixed up in a specified ratio according to the enzymatic assay kit. Then 100µl serum from each of the groups was added to to1000µl of working reagent, The reagent mixture was mixed well and incubated for 60 Seconds.

and aspartate transaminase (AST). This amino-transferase catalyzes the inter-conversion of aspartate and α-ketoglutarate to oxaloacetate and glutamate in the biological system (Singh et al., 2011). An increase in ALT and AST activities in plasma indicates liver dysfunction (Hyder et al., 2013).
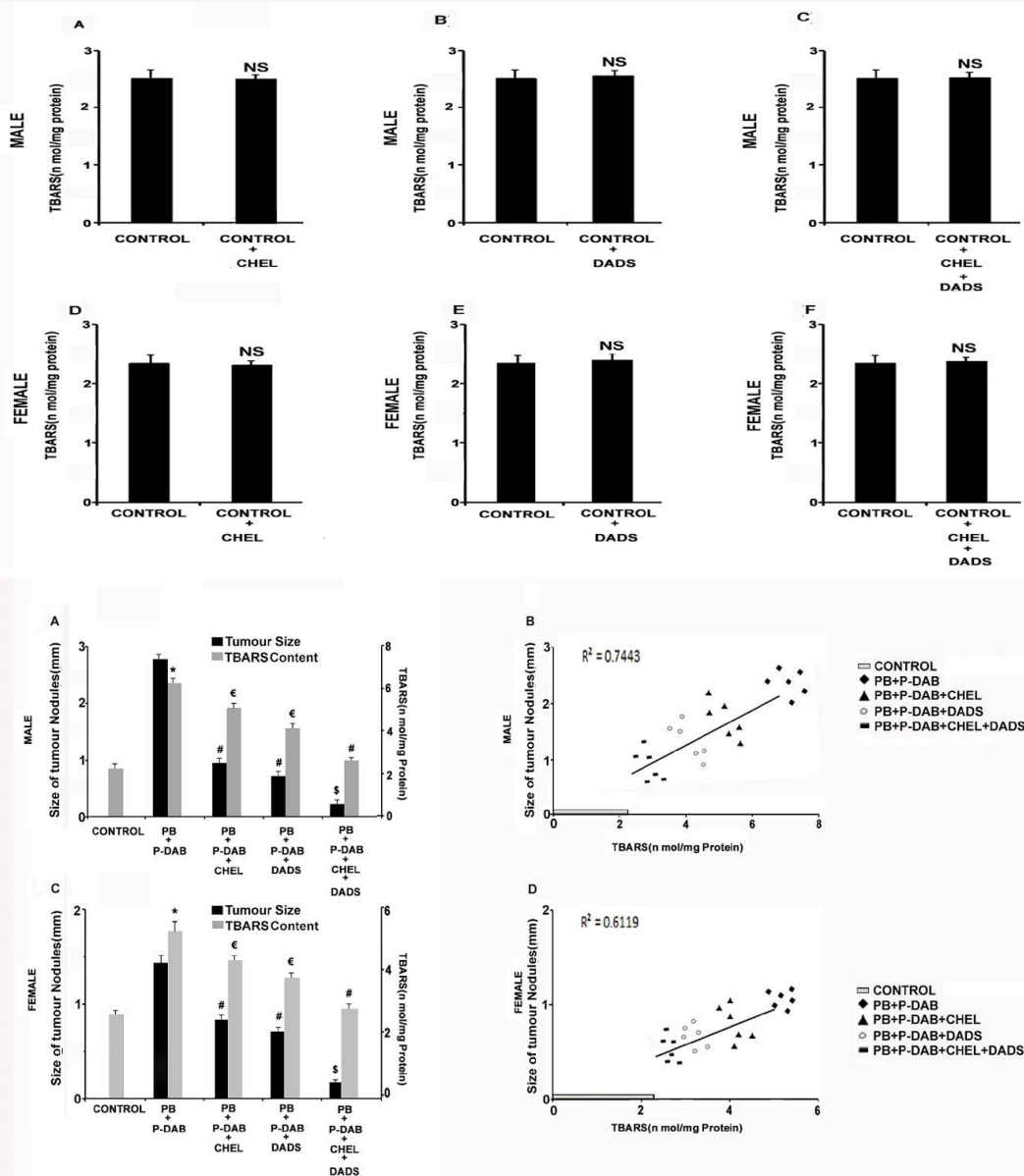
Figure 4 & 5. Toxicity testing of the effective dose of DADS and chelerythrine. To quantify the TBA reactive substances, 1ml of 10mM Tris–HCl buffer (pH 7.4) was added to 0.4mg of membrane protein (in 0.9% saline, pH 7.4). Then 2ml TBA–TCA reagent was added, and the reaction mixture was boiled for 15 min. The aqueous supernatant was isolated after centrifugation, and absorbance was measured at 532nm. The effect of individual chelerythrine (A: male, D: female) and DADS (B: male, E: female) as well as for the combined drug (C: male, F: female), were estimated. NS against control animals.

The data showed enhanced ALT and AST activities in female (Figure 3C and G) and male (Figure 3A and E) mice after PB+P-DAB exposure. Compared to the carcinogen-exposed group, co-treatment with DADS and chelerythrine individually maintained these enzymatic activities to a certain level. The combination of DADS and chelerythrine effectively reduced the activities of such enzymes towards the basal level concerning control mice (Figure 3A, 3C, 3E, and 3G). Correlation analysis suggested a direct impact of tumor development on liver physiology, as depicted by the increased plasma ALT (Figure 3B: $R^2=0.8665$ in male and Figure 3D: $R^2=0.5661$ in female mice) and AST (Figure 3F: $R^2=0.91$ in male mice and Figure 3H; $R^2=0.83$ in female mice) activities. A close correlation of tumor number with plasma AST and ALT activities is more significant in male mice (Figure 3B and F) than in the corresponding female group (Figure 3D and H) after carcinogen exposure, confirming the susceptibility of male mice to chemically induced hepatocarcinoma. Reduction in enzymatic activities concomitant with the protection from tumor development after DADS and

chelerythrine co-treatment, individually and specifically in combination, further demonstrated the efficacy of drug treatment against carcinogenic exposure (Figure 3A, 3B and 3E, 3F).

Absorbance was measured at 320nm for 30-sec intervals up to 2 min. Values were portrayed in U/L. ALT activity and tumor size (mm) of respective drug-treated (individual and combined) and untreated groups of mice were exhibited in the bar diagram. Co-relational impact was analyzed and depicted in the diagram for male (B) and female (D) animals. In AST assay similarly, 100µl serum from the respective experimental group was added to to1000µl of working reagent, mixed well, and incubated for 60 sec. Absorbance was measured at 320nm for 30 sec intervals to 2 min. Data was calculated in U/L.AST activity along with tumor size (mm) of relative groups in the presence or absence of drugs (individual and combined) were shown in male (E) and female (G) mice. Co-relative impacts were expressed in the diagram between AST activity and tumor size of male (F) and female (H) mice groups. The shaded area represented the control value of the experiment. *p<0.01 vs control, €p<0.05, #p<0.02 and $p<0.01 vs PB+P-DAB exposed group.

Toxicity testing of the effective dose of DADS and chelerythrine

In addition to the impactive association with the regulation of disease states, there is clear evidence of drug-induced oxidative stress as a mechanism of toxicity in numerous tissue and organ systems, including the liver, kidney, ear, cardiovascular, and nervous systems during the treatment of several diseases (Kim and Shin, 2014). Well-characterized drugs associated with adverse effects like induction of oxidative stress may contribute to cancer therapeutics (Manda et al., 2009). Thus, TBARS level, a specific indicator of lipid oxidation, was estimated in the control animal after stipulated treatment with the effective dose of 100mg/kg body weight of DADS and 5mg/kg body weight of chelerythrine for 120 days. Individual (Figure 4B and Figure 4A and D) and combined (Figure 4C and F) treatment of DADS and chelerythrine exhibited no significant change in the TBARS content both in male (Figure 4A, 4B, 4C) and female (Figure 4D, 4E, 4F) mice.

Relationship between TBARS content and tumor development in PB+P-DAB exposed mice

Enhanced activity of AST and ALT in the plasma is a well-known marker of the release of enzymes after the generation of stress in the liver (Singh et al., 2011).

Increased activity of AST and ALT instigated us to study the level of TBARS, the signal of cellular oxidation, in the carcinogen-exposed group. PB+P-DAB exposure induced a noteworthy increase in TBARS levels in parallel to the development of tumors in females (Figure 5C) and significantly in males (Figure 5A) mice. DADS and chelerythrine individual co-treatment sufficiently kept up while in combination retained the TBARS level almost similar to control mice both in male (Figure 5A) and female (Figure 5C) counterparts. Correlational analysis between TBARS levels and tumor size (mm) suggested an attentive role of TBARS in tumor development. A distinct relation (Figure 5B: R^2=0.7443) in male mice further suggested the generation of stress and the efficiency of DADS and chelerythrine in protecting liver tissue from that independent variable after carcinogen exposure. Female mice also showed a definite correlation (Figure 5D: R^2=0.6119) and recommended the dependency of tumor development upon stress generation as drug treatment efficiently prevented the development of tumors after inhibiting TBARS synthesis during PB+P-DAB exposure.

Determination of the correlation between TBARS content and tumor development after DADS and chelerythrine co-treatment in PB+P-DAB exposed mice. Tumour nodular size(mm) and TBARS content of the respective drug co-treated (individual or combined group) and untreated group of PB+P-DAB exposed mice in male (A) and female (C) mice. The correlation between tumor size (mm) and TBARS content was calculated and graphically represented for male (B) and female (D) mice. *p<0.01 vs control, €p<0.05, #p<0.02, $p<0.01 vs PB+P-DAB exposed group.

Chromosomal anomalies due to PB+P-DAB exposure and restoration of morphology by the co-treatment of DADS and chelerythrine in mice

Chromosomal abnormalities are a frequent feature of cancer. The analysis of this structural aberration helps to determine the etiology and prognosis of the disease. Morphological abnormalities of chromosomes in cancer cells mostly include loss or gain of chromosomes, chromosomal breakage, stickiness, etc. These changes were summed up following microscopical address and were represented in the percentage of chromosomal abnormalities. PB+P-DAB exposure significantly induced chromosomal abnormalities in females (Figures 6C and G) and more significantly in males (Figures 6A and E) in parallel to an increase in size (mm)(Figure 6A and C) as well as several tumor nodules/4x4mm^2(Figure 6E and G).DADS and chelerythrine individual co-treatment effectively guarded liver tissue from
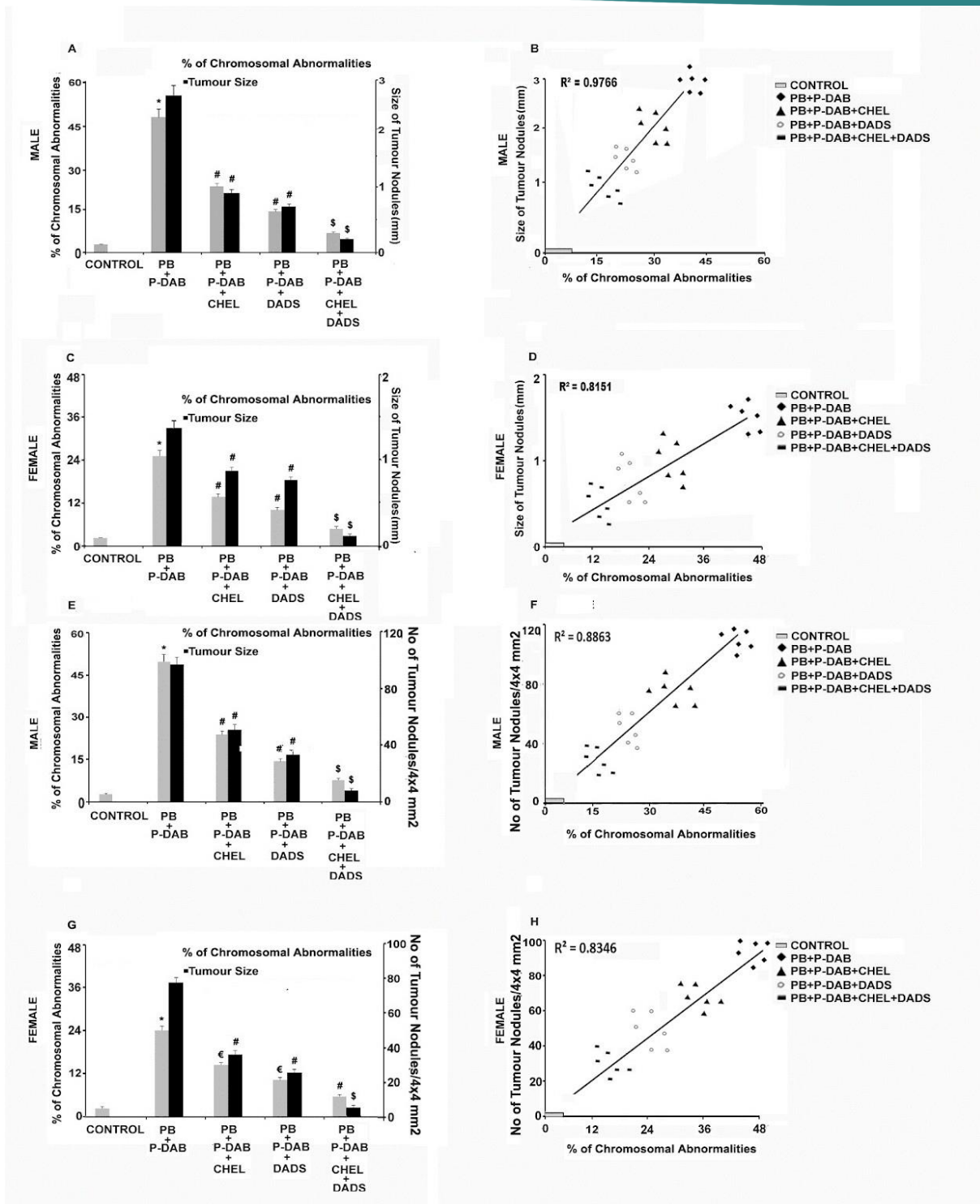
Figure 6. Effect of PB+P-DAB exposure for the generation of Chromosomal abnormalities in DADS and chelerythrine co-treated and untreated group of mice. Mice were intraperitoneally injected with 0.04%.

chemically induced tumor generation (Figure 6A, 6C, 6E, 6G). Although combined treatment of DADS and chelerythrine showed significant protection both in male (Figure 6A and E) and female (Figure 6C and G) groups as depicted by more or less similar levels of chromosomal abnormalities concerning control mice. Relative values of chromosomal abnormalities with their respective tumor size (Figure 6B: $R^2=0.9766$) and tumor number/4x4mm^2 tissue surface area (Figure 6F: R2=0.)8863) demonstrated a significant correlation in treated and untreated groups of male mice. Efficient correlation between the percentage of chromosomal abnormalities with tumor size (mm) (Figure 6D: $R^2=0.8151$) and tumor

in percentage of chromosomal abnormalities. A relationship was described between tumor indices with the generation of chromosomal abnormalities. Association of size of the tumor (mm) with the percentage of chromosomal abnormalities in drug co-treatment (individual and combined) and an untreated group of PB+P-DAB exposed male (A) and female (C) mice. Also, changes in tumor nodules /4x4 mm^2 in parallel to the percentage of chromosomal abnormalities were demonstrated in a drug-co-treated (individual and combined) and untreated group of PB+P-DAB exposed male (E) and female (G) mice. The direct relationship between the size of tumor nodules and the percentage of
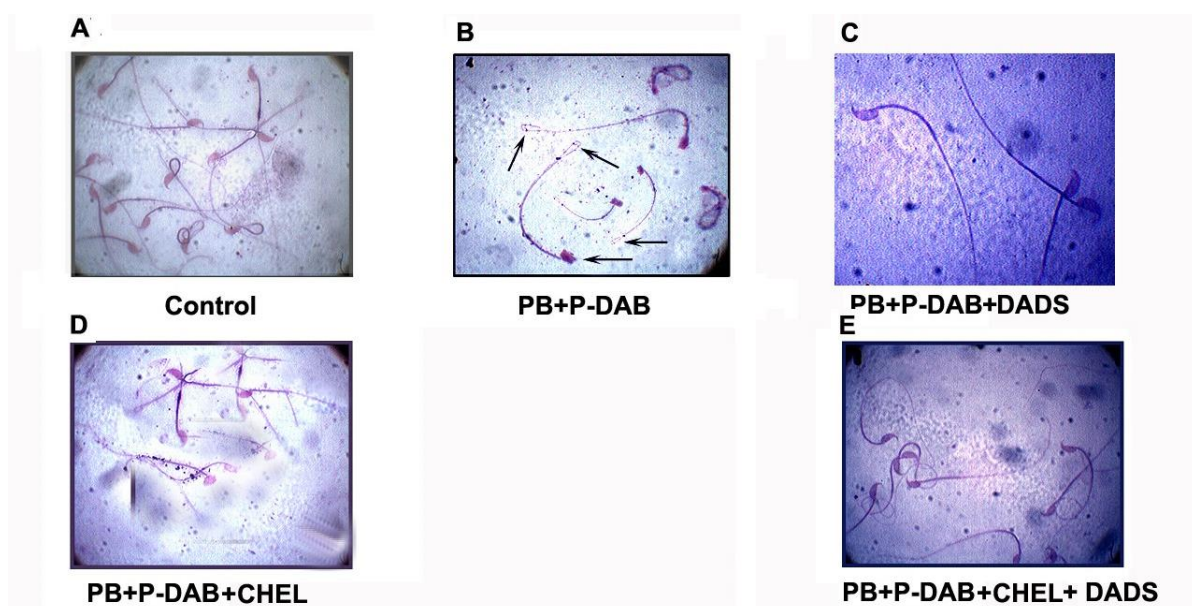
Figure 7. Morphological change in sperm head due to PB+P-DAB exposure and its protection in the DADS and chelerythrine co-treated (individual and combined) group. In the experimental analysis for the determination of sperm head anomalies (SHA), the epididymis was dissected, and its inner content was squeezed out into 0.87% normal saline. Finally, the content was thoroughly cleared, filtered through a silken cloth, and dropped onto grease-free clean slides. The slides were allowed to air dry and stained by dilute Giemsa. The sperm head morphology after microscopic observation in control (A), PB+P-DAB exposed (B), individual DADS (C), and Chelerythrine (D), as well as the combined group (E), was portrayed. Representative results from ten independent animals from each group were exhibited.

number/4x4mm^2 tissue surface area (**Figure 6H**: $R^2=0.8346$) in a drug-treated and untreated group of female mice, they were further confirmed about the direct relationship between chromosomal aberration and tumor development.colchicine solution was sacrificed within 45-60 minutes of injection and femurs were dissected out. Bone marrow was flushed with prewarmed 0.9% KCl solution and the mixture was incubated in a water bath at 37^{0}C for 10 min. Next mixture was centrifuged for 10 min at 1000 rpm and the pellet was fixed with aceto-alcohol (1:3). Slides were prepared by conventional flame dye technique followed by Giemsa staining. Morphological chromosomal abnormalities were summed up and data were represented

chromosomal abnormalities was represented in the respective groups of male (B) and female (D) mice. Correlation between the number of tumor nodules /4x4 mm^2 and the percentage of chromosomal abnormalities was described in the respective group of male (F) and female (H) mice. *$p<0.01$ vs control, €$p<0.05$, #$p<0.02$ and $p<0.01$ vs PB+P-DAB exposed group.

Morphological change in sperm head due to PB+P-DAB exposure and its protection in DADS and chelerythrine co-treatment

Already represented data suggested that male mice were more prone to the development of tumors after PB+P-DAB exposure. Therefore, investigators were

instigated to conduct a study on sperm head anomalies (SHA), which is an indicator of mutagenic potency. PB+P-DAB exposure showed a distinct change in the sperm head concerning the control animal (Figure 7B).DADS and chelerythrine individually reduced the carcinogenic effect to some extent as observed by the reduction in anomalies in Figure 7C and Figure 7D, respectively. Treatment with combined drugs significantly attenuated impactive anomalies regarding sperm head morphology even after PB+P-DAB exposure, as expressed in Figure 7E.

Discussion

Hepatocellular carcinoma is primary liver carcinoma associated with unregulated growth and proliferation of hepatocytes (Kitisin et al., 2007). It has already been reported that HCC is predominant in males and is the commonest in subjects over 40, although it can also be observed in younger people (Farhi et al., 1983). The prognosis is generally poor. The causes of more than 85% of HCC cases are Hepatitis B and C infections, aflatoxin B1 (a carcinogenic toxicant), ethanolic exposure, as well as metabolic disorders (Thorgeirsson and Grisham, 2002). Based on this theoretical foundation, we exposed Swiss albino mice (*Mus musculus) to* Phenobarbital and para dimethyl amino-azobenzene to generate chemically induced hepatocarcinoma.

Our study revealed that it could contribute to genotoxic para-dimethyl amino-azobenzene (P-DAB) and the promoter phenobarbital (PB) led to the effective generation of hepatocellular cytotoxicity, liver tumor formation associated with morpho-chromosomal abnormality, sperm head anomalies, and changes in histological structure. Exposure to P-DAB produces reactive electrolytes (Ohnishi et al., 2001) and reactive oxygen species (ROS). The hepatotoxic effects of ROS play an important role in the initiation and promotion of cells towards neoplastic growth (Ho et al., 2001). Thus, a series of peroxidative reactions lead to the destruction of lipids, which leads to the formation of TBARS, an indicator of cellular toxicity that may affect the membrane molecular structure (Biswas and Khuda-Bukhsh, 2004). ROS accumulation plays a significant role in the generation of DNA mutation. This, in turn, in association with the covalent binding of carcinogenic metabolites to the DNA, probably leads to the formation of liver tumors after PB+P-DAB exposure (Biswas and Khuda-Bukhsh, 2004). Experimentally, morphological studies revealed the enhancement of tumorigenic growth after PB+P-DAB exposure.

Moreover, exposure to carcinogens pointed out a remarkable change in male mice considering the tumor development and biochemical modulation from their contemporary female group of hepatocarcinoma.

Different therapeutics are available for ameliorating hepatocellular carcinoma, such as resection and radiofrequency ablation (RFA), but they likely offer only 5-year survival rates (Biswas and Khuda-Bukhsh, 2002, 2004). Others are Liver transplantation, but it leads to poor survival rates. While trans-arterial chemoembolization (TACE) directs to a 23% improvement in the 2-year survival compared to conservative therapy (Abdalla et al., 2004). Less utilized methods, such as minimally invasive percutaneous treatments and transarterial embolization/chemoembolization, are associated with adverse events, including ischemic cholecystitis, nausea, vomiting, and abdominal pain (Vogl et al., 2009). It has been reported that chemotherapeutics have some adverse bystander effects, which are linked to immunosuppression, fatigue, and gastrointestinal distress, including nausea and vomiting, nephrotoxicity, ototoxicity, and infertility. The situation warrants consideration of alternative therapy, which has already shown some positive results and reduced side effects in ameliorating hepatocellular carcinoma (Brown, 2006). We aimed to determine the efficacy of combining tissue-protective herbal drugs with traditional medicine in restoring normal cell physiology of liver tissue, considering PB+P-DAB-exposed Swiss albino mice as a model for *in-vivo* studies.

It has been reported that crude extract and active purified components of *Chelidonium majus* can exhibit anti-inflammatory, antiviral, antitumor, and antimicrobial properties (Biswas et al., 2005). According to experimental observations, garlic possesses many bio-physiological activities such as antimicrobial, antihypertensive, immunomodulatory, radio-protective, and anticancer activities (Amagase et al., 2006). Reports suggest that garlic has a powerful anti-oxidative defense system and can attenuate intracellular oxidative stress. Among various garlic components, garlic oil and organosulphur effectively increased the activities of GST and GSH reductase (Wu et al., 2001). In our study, initially, control animals were given 100mg/kg body weight DADS and 5mg/kg body weight chelerythrine, and the results did not show any toxic impact after the stipulated 120 days of treatment. Therefore, PB+P-DAB exposed mice were co-treated with 100 mg/kg body weight DADS and 5mg/kg body weight chelerythrine individually as well as in combination to compare the

effectiveness of the therapeutic schedule. Treatment with DADS and chelerythrine, especially in combination, successfully attenuated the carcinogenic growth. A combination of drugs demonstrated effective reduction in acid and alkaline phosphatase and enzymatic activities of other assays like AST, ALT, and GGT as the marker of liver function concerning individual treatment. Retention of sperm head morphology and chromosomal structure, including histological liver tissue configuration, were noted in the chelerythrine and DADS co-treated group. Combinatorial drug treatment was most effective in this perspective, concerning individual co-treatment with chelerythrine and DADS in PB+P-DAB exposed mice. Therapy with drugs maintained morphological, histological and biochemical characteristics towards control levels similarly in both male and female mice, even after carcinogenic exposure.

Therefore, the efficacy of the combination of drugs suggested the study of their mechanism against carcinogenic exposure. It was assumed that the combined drugs might have an additive impact on regulatory influence on certain molecular signalling associated with required protection against chemically induced hepatocarcinoma. Finally, it is imperative to conduct an experimental analysis to explore the efficacy of combined drugs in the amelioration of liver tissue carcinoma following post-treatment therapeutics.

Conflict of interest

The authors declare that they have no conflicts of interest regarding this work.

References

Abdalla, E.K., Vauthey, J.N., Ellis, L.M., Pollock, R., Broglio, K.R., Hess, K., & Curley, S.A. (2004). Recurrence and outcomes following hepatic resection, radiofrequency ablation, and combined resection/ablation for colorectal liver metastases. *Ann. Surg.*, *239*(6), 818-825. https://doi.org/10.1097/01.sla.0000128305.90650.71

AL-Auqbi, T.F.R., & Al-Khalidy, N.T. (2012). The inhibitory effect of oxadiazole and thiadiazoles in vitro on serum alkaline phosphatase enzyme of pregnant women. *Al Mustansiriyah Journal of Harmaceutical Sciences*, *11*(1), 1-8. https://doi.org/10.32947/ajps.v11i1.224

Amagase, H., Petesch, B.L., Matsuura, H., Kasuga, S., & Itakura, Y. (2001). Intake of garlic and its bioactive components. *J. Nutr.*, *131*, 955S–962S. https://doi.org/10.1093/jn/131.3.955S

Andrade, L.J.D.O., D'Oliveira, A., Melo, R.C., Souza, E.C.D., Costa-Silva, C.A., & Parana, R. (2009). Association between Hepatitis C and Hepatocellular Carcinoma. *J. Glob. Infect. Dis.*, *1*(1), 33–37. https://doi.org/10.4103/0974-777X.52979

Bhattacharya, S., & Khuda-Bukhsh, A.R. (2004). The protective action of an antioxidant (L-Ascorbic acid) against genotoxicity and cytotoxicity in mice during p-DAB-induced hepatocarcinogenesis. *Indian J. Cancer.*, *41*(2), 72-80. https://doi.org/10.4103/0019-509X.12349

Biswas, S.J., & Khuda-Bukhsh, A. (2002). Effect of a homeopathic drug, Chelidonium, in amelioration of p-DAB induced hepatocarcinogenesis in mice. *BMC Complement Altern Med.*, *2*(4), 1-12. https://doi.org/10.1186/1472-6882-2-4

Biswas, S.J., & Khuda-Bukhsh, A.R. (2004). Ameliorating effect of an antioxidant (L-ascorbic acid) during p-DAB induced hepatocarcinogenesis in mice: a time course study. *Indian J. Cancer, 41*, 79-87.

Biswas, S.J., Pathak, S., Bhattacharjee, N., Das, J.K., & Khuda-Bukhsh, A.R. (2005). Efficacy of the potentized homeopathic drug, Carcinosin 200, fed alone and in combination with another drug, Chelidonium 200, in amelioration of p-dimethylamino azobenzene-induced hepatocarcinogenesis in mice. *J. Altern. Complement. Med.*, *11*(5), 839-854. https://doi.org/10.1089/acm.2005.11.839

Brown, K.S. (2006). Chemotherapy and other systemic therapies for hepatocellular carcinoma and liver metastases. *Semin. Intervent. Radio.*, *23*(1), 99–108. https://doi.org/10.1055/s-2006-939845

Chatterjee, S., Patra, D., Ghosh, P., Banerjee, S., Chakraborty, P., Chowdhury, K. D., Basu, A., & Sadhukhan, G. C. (2021). Combinational Impact of Chelerythrine and s-allyl Cystine on Melanoma Liver Metastasis: an in vivo Analysis. *Biosc. Biotech. Res. Comm., 14*(1). http://dx.doi.org/10.21786/bbrc/14.1/45

El-Serag, H.B. (2012). Epidemiology of Viral Hepatitis and Hepatocellular Carcinoma. *Gastroenterology*, *142*(6), 1264–1273. https://doi.org/10.1053/j.gastro.2011.12.061

Farhi, D.C., Shikes, R.H., Murari, P.J., & Silverberg, S.G. (1983). Hepatocellular carcinoma in young people.

Feliberti, E.C., & Wagman, L.D. (2006). Radiofrequency ablation of liver metastases

from colorectal carcinoma. *Cancer Control*, *13*(1), 48-51. https://doi.org/10.1177/107327480601300107

Fielding, L. (2006). Current Imaging Strategies of Primary and Secondary Neoplasms of the Liver. *Semin Intervent Radiol., 23*(1), 3–12. https://doi.org/10.1055/s-2006-939836

Gomes, M.A., Priolli, D.G., Tralhão, J.G., & Botelho, M.F. (2013). Hepatocellular carcinoma: epidemiology, biology, diagnosis, and therapies. *Rev. Assoc. Med. Bras., 59*(5), http://dx.doi.org/10.1016/j.ramb.2013.03.005

Ho, J.C., Zheng, S., Comhair, S.A.A., Farver, C., & Erzurum, S.C. (2001). Differential expression of manganese superoxide dismutase and catalase in lung cancer. *Cancer Res., 61*, 8578-8585.

Hyder, M.A., Hasan, M., & Mohielde, H.A. (2013). Comparative Levels of ALT, AST, ALP, and GGT in Liver-associated Diseases. *Eur. J. Exp. Biol., 3*(2), 280-284.

Kim, J., & Shin, M. (2014). An integrative model of multi-organ drug-induced toxicity prediction using gene-expression data. *BMC Bioinformatics*, *15*(Suppl 16), S2, 1-9.

https://doi.org/10.1186/1471-2105-15-S16-S2

Kitisin, K., Pishvaian, M.J., Johnson, L.B., & Mishra, L. (2007). Liver Stem Cells and Molecular Signaling Pathways in Hepatocellular Carcinoma. *Gastrointest Cancer Res., 1*(4 Suppl 2), S13-21.

Kmieć, Z. (2001). Cooperation of liver cells in health and disease. *Adv. Anat. Embryol. Cell Bio., 161*, III-XIII, 1-151. https://doi.org/10.1007/978-3-642-56553-3_1

Kulkarni, N., Tank, S., Korlekar, P., Shidhaye, S., & Barve, P. (2023). A review of gene mutations, conventional testing and novel approaches to cancer screening. *International Journal of Experimental Research and Review*, *30*, 134-162. https://doi.org/10.52756/ijerr.2023.v30.015

Manda, G., Nechifor, M.N., & Neagu, M.T. (2009). Reactive Oxygen Species, Cancer, and Anti-Cancer Therapies. *Curr. Chem. Biol., 3*, 342-366. https://doi.org/10.2174/187231309787158271

Madhu, N.R., Sarkar, B., Roychoudhury, S., Behera, B.K. (2022). Melatonin Induced in Cancer as a Frame of Zebrafish Model. © Springer Nature Singapore Pte Ltd. 2022, S. Pathak et al. (eds.), Handbook of Animal Models and its Uses in Cancer Research, pp. 1-18.

https://doi.org/10.1007/978-981-19-1282-5_61-1

Marszałek, M. (2000). Experimental hepatocarcinogenesis--evaluation of the significance of theoretical models. Contemporary models. *Postepy. Hig. Med. Dosw., 54*(1), 67-82.

Mehta, V., Dey, A., Thakkar, N., Prabhakar, K., Jothimani, G., & Banerjee, A. (2023). Anti-cancer Properties of Dietary Supplement CELNORM against Colon and Lung Cancer: An in vitro preliminary study. *International Journal of Experimental Research and Review*, *32*, 1-14. https://doi.org/10.52756/ijerr.2023.v32.001

Moon, C.S., Moon, D., & Kang, S.K. (2022). Aquaporins in Cancer Biology. Front Oncol. 12, 782829.

https://doi.org/10.3389/fonc.2022.782829.

Ohnishi, S., Murata, M., Degawa, M., & Kawanishi, S. (2001). Oxidative DNA Damage Induced by an N-Hydroxy Metabolite of Carcinogenic 4-Dimethylaminoazobenzene. *Jpn. J. Cancer Res., 92*, 23–29. https://doi.org/10.1111/j.1349-7006.2001.tb01043.x

Petruczynik, A., Plech, T., Tuzimski, T., Misiurek, J., Kaproń, B., Misiurek, D., Szultka-Młyńska, M., Buszewski, B., & Waksmundzka-Hajnos, M. (2019). Determination of Selected Isoquinoline Alkaloids from *Mahonia aquifolia; Meconopsis cambrica; Corydalis lutea; Dicentra spectabilis; Fumaria officinalis; Macleaya cordata* Extracts by HPLC-DAD and Comparison of Their Cytotoxic Activity. *Toxins.* 2019; 11(10):575. https://doi.org/10.3390/toxins11100575

Rami, N., Kulkarni, B., Chibber, S., Jhala, D., Parmar, N., & Trivedi, K. (2023). In vitro antioxidant and anticancer potential of Annona squamosa L. Extracts against breast cancer. *International Journal of Experimental Research and Review*, *30*, 264-275.

https://doi.org/10.52756/ijerr.2023.v30.024

Saha, A., & Yadav, R. (2023). Study on segmentation and prediction of lung cancer based on machine learning approaches. *International Journal of Experimental Research and Review*, *30*, 1-14. https://doi.org/10.52756/ijerr.2023.v30.001

Singh, A., Bhat, T.K., & Sharma, O.P. (2011). Clinical Biochemistry of Hepatotoxicity. *J. Clin. Toxicol., 4*, 914–917.

Thorgeirsson, S.S., & Grisham, J.W. (2002). Molecular pathogenesis of human hepatocellular carcinoma. *Nat. Genet., 31*, 339-346. https://doi.org/10.1038/ng0802-339

Vogl, T.J., Gruber, T., Balzer, J.O., Eichler, K., Hammerstingl, R., & Zangos, S. (2009). Repeated transarterial chemoembolization in the treatment of liver metastases of colorectal cancer: prospective study. *Radiology*, *250*(1), 281-289. https://doi.org/10.1148/radiol.2501080295

Wangensteen, K.J., Wang, Y.J., Dou, Z., Wang, A.W., Mosleh-Shirazi, E., Horlbeck, M.A., Gilbert, L.A., Weissman, J.S., Berger, S.L., & Kaestner, K.H. (2018). Combinatorial genetics in liver repopulation and carcinogenesis with a in vivo CRISPR activation platform. *Hepatology*, *68*(2), 663-676. https://doi.org/10.1002/hep.29626.

Wu, C.C., Sheen, L.Y., Chen, H.W., Tsai, S.J., & Lii, C.K. (2001). Effects of organosulfur compounds from garlic oil on the antioxidation system in rat liver and red blood cells. *Food Chem. Toxicol.*, *39*, 563–569. https://doi.org/10.1016/S0278-6915(00)00171-X

Xu, X.S., Wan, Y., Song, S.D., Chen, W., Miao, R.C., Zhou, Y., Zhang, L.Q., Qu, K., Liu, S.N., Zhang, Y.L., Dong, Y.F., Liu, C. (2014). Model based on γ-glutamyltransferase and alkaline phosphatase for hepatocellular carcinoma prognosis. *World J. Gastroenterol.*, *20*(31), 10944-10952. https://doi.org/10.3748/wjg.v20.i31.10944